Fuel xxx (2014) xxx–xxx

Contents lists available at ScienceDirect

Fuel

journal homepage: www.elsevier.com/locate/fuel

Short communication

Pressure-controlled advanced distillation curve analysis and rotational viscometry of swine manure pyrolysis oil ☆

Q1 Peter Y. Hsieh, Thomas J. Bruno *

National Institute of Standards and Technology, Material Measurement Laboratory, Applied Chemicals and Materials Division, 325 Broadway MS 647.07, Boulder, CO 80305, USA

ARTICLE INFO

Article history:
Received 11 February 2014
Received in revised form 27 March 2014
Accepted 10 April 2014
Available online xxxx

Keywords:
Bio-oil
Composition-explicit distillation
Pyrolysis oil
Swine manure
Viscosity

ABSTRACT

Pyrolysis is an effective method of converting agricultural byproducts to a tarry complex fluid suitable for use as a liquid fuel. While superficially similar in appearance to crude petroleum, pyrolysis oil contains significantly more oxygenated and nitrogenous compounds and up to 30% water by mass. These differences in composition affect both the heating value and viscosity of the fuel. We used the reduced-pressure advanced distillation curve (ADC) method to characterize the boiling point and composition of pyrolysis oil derived from swine manure. The swine manure pyrolysis oil was found to contain ~15% water by mass. Thermal cracking of the sample was observed near 300 °C at 3.5 kPa. The pyrolysis oil viscosity decreases exponentially as a function of temperature from 50 to 75 °C.

1. Introduction

Over the past century, widespread adoption of petroleum-based fuels has transformed industrial economies around the world. Conventional petroleum is readily extracted, transported, and refined into a wide range of fuels. Recent concerns over the rising cost of conventional petroleum extraction due to diminishing reserves and the environmental effects of fossil fuel combustion have spurred a search for renewable sources of liquid fuels suitable for heating and transportation. Pyrolysis, or the breakdown of organic compounds at high temperatures in the absence of oxygen, is a promising approach to producing liquid fuels from a wide range of biomass sources [1]. Compared with first-generation biofuels, pyrolysis oils have higher energy density and do not compete with food crop production. Increased use of renewable liquid fuels is an energy policy objective of both the United States and the European Union [2,3].

The introduction of ASTM D7544, a standard specification for pyrolysis liquid biofuel used in industrial burners, marks an important milestone in the acceptance of pyrolysis oil as a renewable fuel [4]. The specification defines the heat of combustion, composition, kinematic viscosity, density, flash point, and pour point of grade D and G pyrolysis oils suitable for use in industrial burners.

While pyrolysis oil appears promising for meeting future energy needs, present methods of production yield a product that cannot be blended with petroleum-based transportation fuels. Means of separating, characterizing and upgrading pyrolysis oil are actively being sought today [5,6].

Archeological evidence shows that destructive distillation of wood, a form of slow pyrolysis, was used to obtain wood tar, a pyrolysis oil product, as early as the Paleolithic era [7]. The development of fast pyrolysis reactors in recent times has improved the yield of pyrolysis oil relative to pyrolysis gas and solid char formed from biomass [8]. Pyrolysis oil can be produced from a wide range of feedstocks, including waste products from timber production or agriculture [9–11]. Agricultural waste offers a ready supply of renewable biomass for pyrolysis oil production. Using agricultural waste to produce pyrolysis oil also reduces the environmental impact of contemporary intensive farming practices.

Intensive farming often generates concentrated waste products that can overwhelm local ecosystems if they are left untreated prior to disposal. One such example is swine manure slurries from large-scale feedlot operations [12]. The conversion of swine manure slurry to pyrolysis oil can simultaneously reduce the amount of waste that must be treated and produce a material that can be upgraded to fuels and chemicals. Characterizing the changes in the chemical and physical properties of swine manure pyrolysis oil as a function of temperature provides useful data in understanding how pyrolysis oils may be further refined or upgraded to meet future renewable fuel requirements.

☆ Contribution of the National Institute of Standards and Technology. Not subject to copyright in the USA.

* Corresponding author. Tel.: +1 303 497 5158; fax: +1 303 497 6682.
E-mail address: bruno@boulder.nist.gov (T.J. Bruno).

http://dx.doi.org/10.1016/j.fuel.2014.04.039
0016-2361/© 2014 Published by Elsevier Ltd.

Pyrolysis oils, like other complex fluids, are challenging to characterize due to the large number of components that are present. Characterization processes in the laboratory, such as distillation, often have analogous processes in industrial-scale refining. The vapor–liquid equilibrium (VLE) of a complex fluid may be approximated by its volatility during distillation. Distillation of a complex fluid can yield experimental data useful in characterizing its physical and chemical properties.

The advanced distillation curve (ADC) method offers significant advantages over earlier approaches to complex fluid characterization, featuring (1) a composition-explicit data channel for each distillate fraction (for both qualitative and quantitative analyses), (2) temperature, volume and pressure measurements of low uncertainty that are true thermodynamic state points suitable for equation of state development, (3) an assessment of the density and enthalpy as a function of distillate volume fraction, (4) trace chemical analysis of each distillate fraction, and (5) a corrosivity assessment of each distillate fraction [13–15]. ADC data are consistent with a century of literature on the thermophysical properties of complex fluids. The method has been used to characterize *n*-alkanes [16], simple azeotropes [17], gas turbine fuels [18–23], diesel and biodiesel fuels [24–30], gasolines [31–33], rocket propellants [18,34–36], crude oils [37–39], and pyrolysis oils [40]. Unlike the conventional distillation curve, fuel volatility or vapor–liquid equilibrium data, ADC data can be modeled with an equation of state [41–46]. This short communication summarizes the application of the reduced-pressure ADC method to swine manure pyrolysis oil previously characterized at atmospheric pressure [40], and provides additional data in the study of pyrolysis oils.

2. Materials and methods

2.1. Materials

Pyrolysis oil derived from swine manure slurry was provided by Professor Yuanhui Zhang at the University of Illinois at Urbana-Champaign [47–49]. The pyrolysis oil was produced by reacting swine manure slurry with an initial charge of 0.34–2.76 MPa of carbon monoxide at an operating temperature of 275–350 °C in a 1.8 L T316 stainless steel reactor. Additional details of the swine manure slurry preparation and thermochemical conversion process have been published previously [47,50]. The resultant pyrolysis oil has a tar-like appearance and has a strong smoky odor. The sample was stored at ambient temperature and analyzed as received.

The pyrolysis oil is mostly insoluble in *n*-hexane and toluene, but dissolves completely in acetone. The acetone solvent used in this study was purchased from a commercial supplier and determined to be approximately 99% (mass/mass) pure through gas chromatography with mass spectrometric detection (GC–MS).

2.2. Advanced distillation curve method

The reduced-pressure ADC apparatus and sampling method have been described in detail in several earlier works [16,18,20,31,51]; a short description of particular steps used in this study is noted here for clarity. Due to the viscous and opaque nature of the sample, the initial volume of the pyrolysis oil in the boiling flask (kettle) was calculated from its mass and its density at ambient temperature (0.787 g/cm^3, with a combined expanded uncertainty of 0.036 g/cm^3, as measured through pycnometry). The mass of the boiling flask was measured on an analytical balance prior to and after sample introduction; the sample mass was calculated by difference. Estimated uncertainties were added in quadrature to yield the combined expanded uncertainties that are reported in the results and discussion.

Two thermocouples were used to monitor the vapor temperature at the bottom of the distillate take-off position (T_h) in the distillation head and the liquid temperature (T_k) in the kettle concurrently. An aluminum heating enclosure was used to increase the fluid temperature uniformly and at a constant rate using prior distillation data as a guide. The distillate vapor travels from the kettle through the distillation head and enters an air-cooled condenser, where it condenses into a liquid condensate. The liquid condensate then flows through a sampling adapter before entering a volume-calibrated graduated receiver. The distillation curve of the sample is determined by measuring changes in the kettle temperature as a function of distillate volume.

A commercial vacuum controller was connected to the apparatus to measure and control the system pressure. The controller uses a piezoresistive transducer and continuously regulated proportional valves to evacuate and vent the system for pressure control. The pressure controller can maintain a set pressure between 1 and 83 kPa (0.1 kPa resolution, 0.1 kPa estimated uncertainty). Pressure readings were calibrated by measuring the vapor pressure of deionized water as a function of temperature. A liquid nitrogen cold trap was placed between the apparatus and the pressure controller to condense any vapors that might escape the apparatus.

A gas reservoir containing 1 L of carbon dioxide was connected directly to the vacuum controller as a safety measure. The volume of the carbon dioxide gas in the reservoir exceeds the total system volume of the ADC apparatus. If the system must be brought to atmospheric pressure quickly, the carbon dioxide from the reservoir prevents air from coming into contact with the hot pyrolysis oil sample in the boiling flask.

2.3. Gas chromatography with mass spectrometric detection (GC–MS)

Small aliquots (10 μL) of the distillate were withdrawn at predetermined distillate volume fractions with a pressure-balanced chromatography syringe in the receiver adapter hammock and dissolved in a fixed quantity of acetone inside an autosampler vial. The diluted aliquots were analyzed using GC–MS (30 m column with an 250 μm inner diameter coated with a 0.25 μm film of 5% phenyl-95% dimethylpolysiloxane, helium carrier gas at 48.3 kPa or 7 psi inlet pressure, split ratio of 50:1, temperature program starting with an isothermal soak at 75 °C for 1 min, followed by a slow ramp to 275 °C at a heating rate of 5 °C/min and a fast ramp to 305 °C at a heating rate of 15 °C/min) [52]. The fluid components were characterized through mass spectrometric detection and identified using the NIST 11 Mass Spectral Library [53].

2.4. Rotational viscometry

A commercial rotating cylinder viscometer (inner spindle diameter 1.175 cm, outer cylinder diameter 1.900 cm) was used to measure the kinematic viscosity of the bulk fluid at 6 and 12 rpm. The viscometer was calibrated using a certified poly-alpha olefin reference fluid. The bulk pyrolysis oil was first added to an aluminum sample cylinder, which was then loaded into a commercial heating enclosure. The pyrolysis oil was heated to 70.0 °C prior to spindle insertion. Its viscosity was measured as a function of temperature based on multiple steady-state values at 5 °C intervals, as the enclosure temperature was decreased from 70 to 50 °C.

3. Results and discussion

3.1. Boiling point and composition as a function of distillate volume

A typical ADC measurement begins with visual observation of the initial boiling conditions (onset of bubbling, sustained bubbling

Please cite this article in press as: Hsieh PY, Bruno TJ. Pressure-controlled advanced distillation curve analysis and rotational viscometry of swine manure pyrolysis oil. Fuel (2014), http://dx.doi.org/10.1016/j.fuel.2014.04.039

and the rise of vapor into the distillation head). While the onset of bubbling and sustained bubbling temperatures are useful as diagnostics during distillation, the vapor rise temperature is the theoretically significant initial boiling temperature (IBT) of the complex fluid. This temperature is important because the sample composition in the boiling flask is fixed and measurable at the start of the distillation; therefore, the data can be used to develop an equation of state. The measured IBT of the swine manure pyrolysis oil is 31.6 °C (with an expanded uncertainty of 1.0 °C) at 3.5 kPa (with an expanded uncertainty of 1.6 kPa). In comparison, the boiling range of water is 26.67 °C (at 3.5 kPa) and 33.23 °C (at 5.1 kPa) in the pressure range of the measurement as calculated with the Wagner and Pruss equation of state in the NIST REFPROP program [54,55]. The water boiling temperatures from the Wagner and Pruss equation of state have an expanded uncertainty of 1.20 °C. The reduced pressure IBT of the swine manure pyrolysis oil is consistent with the boiling of water present in the pyrolysis oil at 3.5 kPa. The finding is in agreement with the formation of an aqueous distillate phase and Fourier-transform infrared spectroscopy data previously reported by Ott et al. for atmospheric pressure distillation of a similar pyrolysis oil sample [40], which was reported to contain between 11.3% and 15.8% (mass/mass) water [48].

Distillation curve data at reduced pressure (3.5 kPa, with an expanded uncertainty of 1.6 kPa) are shown graphically in Fig. 1; atmospheric pressure distillation curve data from an earlier study is also plotted for comparison [40]. The average atmospheric pressure of the high altitude laboratory at Boulder, CO (1655 m above sea level) is 83.1 kPa. In contrast to the atmospheric pressure distillation, some of the distillate in the reduced pressure distillation is noncondensable at reduced pressure and ambient temperature. Most of the noncondensable distillate fraction is captured in the liquid nitrogen cold trap. To measure the mass and volume of this fraction, the cold trap is allowed to warm to ambient temperature at atmospheric pressure. Up to 3.4 g of distillate mass is uncaptured due to volatilization during thawing of the cold trap and condensation in the vacuum transfer line. The total uncaptured mass is calculated by difference between the initial sample mass and the total recovered mass after distillation. It is added to the mass of the distillate recovered from the cold trap to calculate the offset for the condensable distillate volume. An estimate of the boiling temperature for the noncondensable portion of the distillation curve, based on the offset, IBT, and the boiling temperature at the first condensable distillate drop, is also shown in Fig. 1.

The reduced pressure distillation curve shows a steep increase in boiling temperature from 14.3% to 17.3% distillate volume fraction, increasing from 58.6 to 272.3 °C. The steep rise in boiling temperature can be explained by the removal of water from the sample and the relative lack of distillable compounds in this temperature range. Additional condensable distillate is formed above 272.3 °C due to further thermal cracking of the biogenic compounds (e.g., amino acids, lipids, saccharides) present in the pyrolysis oil. The convergence of the reduced pressure and atmospheric pressure distillation curves above 20% distillate volume fraction indicates that thermal cracking, independent of system pressure, is a significant factor above 300 °C.

GC–MS composition data (Fig. 2) shows that the distillate contains principally trace quantities of pyrazine derivatives at 13.2% distillate volume fraction, but contains a wide variety of biogenic pyrolysis compounds for distillate volume fractions greater than 15% (see Table 1). The composition data also shows that the distillate nitrogen content decreases from 20% to 3% (mass/mass) over

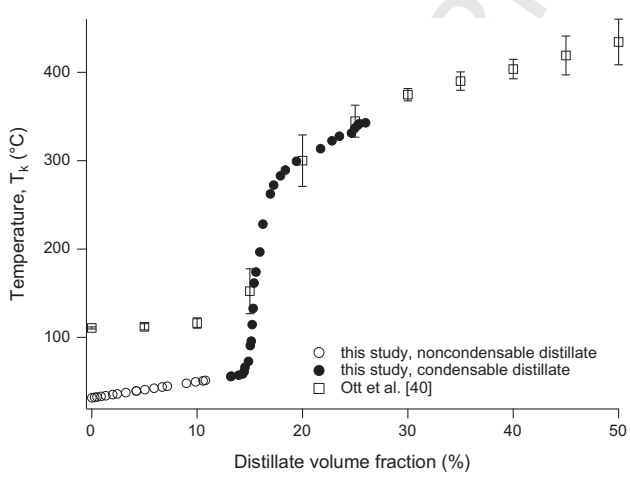

Fig. 1. Distillation curve data for swine manure pyrolysis oil at 3.5 kPa (with an expanded uncertainty of 1.6 kPa), plotted with circles, and 83.1 kPa (□) [40]. Open circles (○) indicate estimated boiling temperatures for the noncondensable distillate recovered from the liquid nitrogen cold trap. Filled circles (●) indicate boiling temperatures for the condensable distillate directly observed in the graduated receiver.

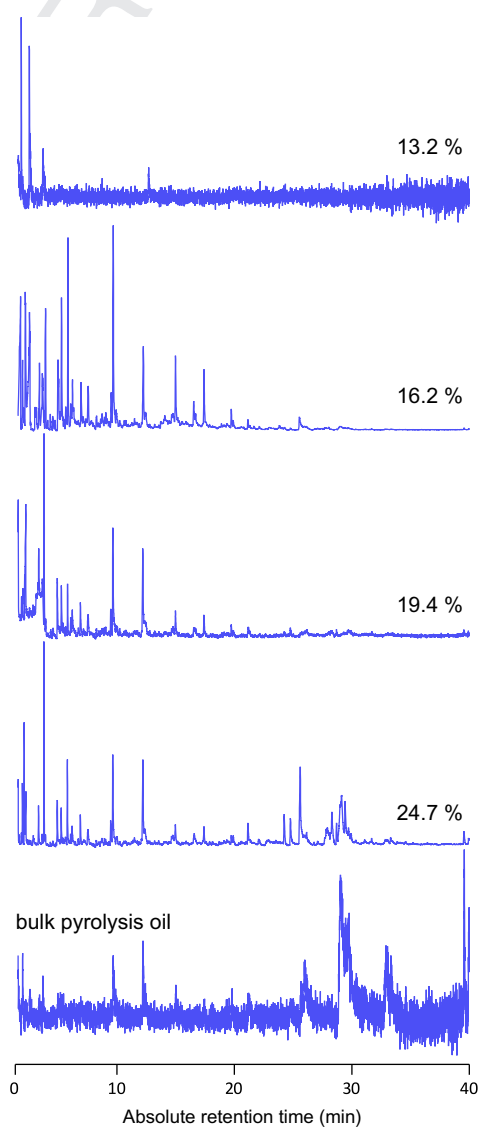

Fig. 2. Chromatograms of swine manure pyrolysis oil distillate fractions, presented in arbitrary units of intensity (based on sum of mass spectrometer signals) plotted as a function of absolute retention time.

Please cite this article in press as: Hsieh PY, Bruno TJ. Pressure-controlled advanced distillation curve analysis and rotational viscometry of swine manure pyrolysis oil. Fuel (2014), http://dx.doi.org/10.1016/j.fuel.2014.04.039

the measurable range of 13.2–24.7% distillate volume fraction. Overall, the nitrogen content of the distillate appears to be closer to swine manure (dry matter basis) [48] than crude oils, which typically contain from 0.01% to 0.9% (mass/mass) nitrogen [56]. The high nitrogen content of the pyrolysis oil is an important factor to consider in refining and blending, as nitrogen is known to degrade fuel stability and processing catalysts. Upgrading of the pyrolysis oil will be an important first step to improve its suitability as a fuel blendstock.

3.2. Dynamic viscosity as a function of temperature

Viscosity is an important fluid property in the design of chemical reactors. In general, pyrolysis oils exhibit Newtonian behavior and their viscosities do not exhibit shear-rate dependence [57]. Fig. 3 shows the change in the dynamic viscosity as a function of temperature of the swine manure pyrolysis oil. Viscosity data reported by He et al. on a similar instrument and sample have been included in Fig. 3 for comparison [48]. Based on the two data sets, the dynamic viscosity (μ) of the swine manure pyrolysis oil as a function of temperature, in the range of 45–75 °C can be described by Eq. (1):

$$\mu(\text{in mPa s}) = 656.54 + 2.4535 \times 10^7 \exp[-0.17885\ T] \quad (1)$$

where T is the temperature in °C. Using Eq. (1), the dynamic viscosity of the swine manure pyrolysis oil is estimated to be 19.8 Pa s at 40 °C. The density of the swine manure pyrolysis oil is 787 kg/m^3 at 20.6 °C. Therefore, the kinematic viscosity of the swine manure pyrolysis oil is at least 25,200 mm^2/s, which is considerably higher than the maximum value permitted by ASTM D7544 (125 mm^2/s at 40 °C) for grade D and G pyrolysis oil fuels [4].

4. Conclusions

We applied the advanced distillation curve method at reduced pressure to a sample of swine manure pyrolysis oil. The distillation curve of the sample is consistent with boiling of residual water and light hydrocarbon compounds, followed by thermal cracking of the biogenic compounds remaining in the pyrolysis oil. GC–MS data

Table 1
Chemical compounds identified with GC–MS in swine manure pyrolysis oil distillate. See text for description of GC–MS parameters. Individual peak areas for each distillate volume fraction were normalized against the sum of all chromatogram peak areas for that distillate volume fraction.

Peak	Retention time (min)	Peak assignment	Empirical formula	Relative molecular mass (g/mol)	Normalized peak areas			
					Distillate volume fraction (%)			
					13.2	16.2	19.4	24.7
1	1.67	Butanoic acid	$C_4H_8O_2$	88		11.4		
2	1.86	Pyrazine, methyl-	$C_5H_6N_2$	94	22.6			
3	1.88	Butanoic acid, 3-methyl-	$C_5H_{10}O_2$	102			1.5	
4	1.96	2-pentanone, 4-hydroxy-4-methyl-	$C_6H_{12}O_2$	116		1.7	2.5	1.9
5	2.16	2-pentanone, 4-amino-4-methyl-	$C_6H_{13}NO$	115		7.4	[a]	3.3
6	2.32	Pentanoic acid	$C_5H_{10}O_2$	102		11.5	14.7	4.5
7	2.57	Pyrazine, 2,5-dimethyl-	$C_6H_8N_2$	108	45.0			
8	3.36	Phenol	C_6H_6O	94		2.3	2.6	1.8
9	3.40	Hexanoic acid	$C_6H_{12}O_2$	116				
10	3.63	2,4-pentanediamine, 2-methyl-	$C_6H_{16}N_2$	116			6.5	0.5
11	3.66	1,3-propanediamine, N,N′,2,2-tetramethyl-	$C_7H_{18}N_2$	130				
12	3.69	Pyrazine, 2-ethyl-6-methyl-	$C_7H_{10}N_2$	122	22.4	4.3		
13	3.83	2,2,5,5-tetramethyl-4-ethyl-3-imidazoline-1-oxyl	$C_9H_{17}N_2O$	169		5.9	13.3	7.9
14	4.33	2-cyclopenten-1-one, 2,3-dimethyl-	$C_7H_{10}O$	110		0.2		
15	4.56	5-ethyl-2-methyl-pyridin-4-amine	$C_8H_{12}N_2$	136		0.2		
16	4.95	p-cresol	C_7H_8O	108		4.8	5.1	2.6
17	5.27	Phenol, 2-methoxy-	$C_7H_8O_2$	124		5.6	5.4	2.1
18	5.64	Pyrazine, (1-methylethenyl)-	$C_7H_8N_2$	120		0.5		
19	5.81	4-piperidinone, 2,2,6,6-tetramethyl-	$C_9H_{17}NO$	155		6.2	3.8	4.1
20	6.07	1H-pyrrole, 2,3,4,5-tetramethyl-	$C_8H_{13}N$	123		0.7	1.5	0.6
21	6.22	2,5-pyrrolidinedione, 1-ethyl-	$C_4H_5NO_2$	99		2.8	3.2	1.2
22	6.92	Phenol, x-ethyl-	$C_8H_{10}O$	122		1.9	3.3	1.9
23	7.54	1H-pyrrole, 2-ethyl-3,4,5-trimethyl-	$C_9H_{15}N$	137				1.4
24	7.55	phenol, 4-(ethylamino)-				2.5		
25	8.26	2,5-pyrrolidinedione, 1-propyl-	$C_4H_5NO_2$	99		0.3		
26	9.49	4-morpholinepropanamine	$C_7H_{16}N_2O$	144		1.4	2.6	1.2
27	9.66	Phenol, 4-ethyl-2-methoxy-	$C_9H_{12}O_2$	152		8.5	13.7	6.2
28	9.83	Propanamide, N-tetrahydrofurfuryl-2-methyl-	$C_9H_{17}NO_2$	171		2.2		
29	12.22	N-[2-hydroxyethyl]-succinimide	$C_6H_9NO_3$	143		4.9	13.9	8.1
30	12.43	1H-Indole-3-propanenitrile, α-amino-	$C_{11}H_{11}N_3$	185		1.4		
31	12.71	Oxalic acid, isobutyl nonyl ester	$C_{15}H_{28}O_4$	272	9.9			
32	14.99	1-pentadecene	$C_{15}H_{30}$	210		4.0	3.4	1.9
33	16.58	1-pentadecene, 2-methyl-	$C_{16}H_{32}$	224		2.3		
34	17.42	Cetene	$C_{16}H_{32}$	224		3.0	3.1	1.4
35	19.74	1-hexadecanol	$C_{16}H_{34}O$	242		0.9		
36	21.16	Benzenebutanal	$C_{10}H_{12}O$	148				1.7
37	24.25	Hexadecanenitrile	$C_{16}H_{31}N$	237				2.7
38	24.78	Hexadecanoic acid, methyl ester	$C_{17}H_{34}O_2$	270				2.3
39	25.59	*n*-hexadecanoic acid	$C_{16}H_{32}O_2$	256		1.2		9.9
40	28.31	Octadecanenitrile	$C_{18}H_{35}N$	265				5.3
41	28.70	Methyl stearate	$C_{19}H_{38}O_2$	298				1.5
42	29.09	*cis*-vaccenic acid	$C_{18}H_{34}O_2$	282				17.5
43	29.45	Octadecanoic acid	$C_{18}H_{36}O_2$	284				5.6
44	39.56	Cholest-4-ene	$C_{27}H_{46}$	370				1.1

[a] Peak overlap.

Please cite this article in press as: Hsieh PY, Bruno TJ. Pressure-controlled advanced distillation curve analysis and rotational viscometry of swine manure pyrolysis oil. Fuel (2014), http://dx.doi.org/10.1016/j.fuel.2014.04.039

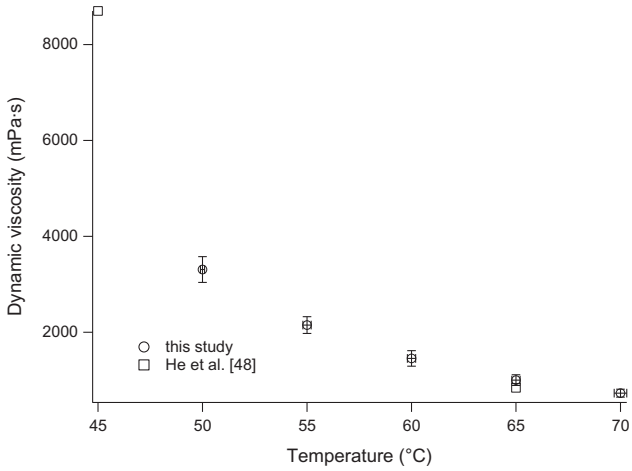

Fig. 3. Dynamic viscosity of swine manure pyrolysis oil plotted as a function of temperature as measured in a temperature-controlled rotational viscometer (○). Viscosity values for a similar pyrolysis oil (□) reported by He et al. are plotted for comparison [48].

showed a significant quantity of nitrogenous compounds present in the distillate, which may pose a problem for refining and blending of the pyrolysis oil. The viscosity of the swine manure pyrolysis oil exceeds limits for use as an industrial burner fuel.

Acknowledgements

This research was performed while Peter Y. Hsieh held a National Research Council Research Associateship Award at NIST. We acknowledge the assistance of Dr. Yuanhui Zhang at the University of Illinois Urbana-Champaign for providing the swine manure-derived pyrolysis oil.

References

[1] Czernik S, Bridgwater AV. Overview of applications of biomass fast pyrolysis oil. Energy Fuels 2004;18:590–8.
[2] Energy Independence and Security Act of 2007. Public Law 110–140; 2007.
[3] European Parliament and of the Council Directive 2003/30/EC. Official Journal of the European Union; 2006, L 123/42-46.
[4] ASTM, D7544-12 Standard specification for pyrolysis liquid biofuel. In: Book of Standards, West Conshohocken, PA; 2012.
[5] Graca I, Lopes JM, Cerqueira HS, Ribeiro MF. Bio-oils upgrading for second generation biofuels. Ind Eng Chem Res 2013;52:275–87.
[6] Capunitan JA, Capareda SC. Characterization and separation of corn stover bio-oil by fractional distillation. Fuel 2013;112:60–73.
[7] Grünberg JM. Middle Palaeolithic birch-bark pitch. Antiquity 2002;76:15–6.
[8] Mohan D, Pittman CU, Steele PH. Pyrolysis of wood/biomass for bio-oil: a critical review. Energy Fuels 2006;20:848–89.
[9] Adebanjo AO, Dalai AK, Bakhshi NN. Production of diesel-like fuel and other value-added chemicals from pyrolysis of animal fat. Energy Fuels 2005;19:1735–41.
[10] Ringer M, Putsche V, Scahill J. Large-scale pyrolysis oil production: a technology assessment and economic analysis. Golden, CO: National Renewable Energy Laboratory; 2006.
[11] Acikalin K, Karaca F, Bolat E. Pyrolysis of pistachio shell: effects of pyrolysis conditions and analysis of products. Fuel 2012;95:169–77.
[12] Honeyman MS. Sustainability issues of US swine production. J Anim Sci 1996;74:1410–7.
[13] Bruno TJ, Ott LS, Smith BL, Lovestead TM. Complex fluid analysis with the advanced distillation curve approach. Anal Chem 2010;82:777–83.
[14] Bruno TJ, Ott LS, Lovestead TM, Huber ML. Relating complex fluid composition and thermophysical properties with the advanced distillation curve approach. Chem Eng Technol 2010;33:363–76.
[15] Bruno TJ, Ott LS, Lovestead TM, Huber ML. The composition-explicit distillation curve technique: relating chemical analysis and physical properties of complex fluids. J Chromatogr A 2010;1217:2703–15.
[16] Bruno TJ. Improvements in the measurement of distillation curves. 1. A composition-explicit approach. Ind Eng Chem Res 2006;45:4371–80.
[17] Hadler AB, Ott LS, Bruno TJ. Study of azeotropic mixtures with the advanced distillation curve approach. Fluid Phase Equilib 2009;281:49–59.
[18] Bruno TJ, Smith BL. Improvements in the measurement of distillation curves. 2. Application to aerospace/aviation fuels RP-1 and S-8. Ind Eng Chem Res 2006;45:4381–8.
[19] Smith BL, Bruno TJ. Composition-explicit distillation curves of aviation fuel JP-8 and a coal-based jet fuel. Energy Fuels 2007;21:2853–62.
[20] Smith BL, Bruno TJ. Improvements in the measurement of distillation curves. 4. Application to the aviation turbine fuel Jet-A. Ind Eng Chem Res 2007;46:310–20.
[21] Smith BL, Bruno TJ. Application of a composition-explicit distillation curve metrology to mixtures of Jet-A and S-8. J Propul Power 2008;24:618–23.
[22] Bruno TJ, Baibourine E, Lovestead TM. Comparison of synthetic isoparaffinic kerosene turbine fuels with the composition-explicit distillation curve method. Energy Fuels 2010;24:3049–59.
[23] Burger JL, Bruno TJ. Application of the advanced distillation curve method to the variability of jet fuels. Energy Fuels 2012;26:3661–71.
[24] Ott LS, Smith BL, Bruno TJ. Composition-explicit distillation curves of mixtures of diesel fuel with biomass-derived glycol ester oxygenates: a fuel design tool for decreased particulate emissions. Energy Fuels 2008;22:2518–26.
[25] Ott LS, Bruno TJ. Variability of biodiesel fuel and comparison to petroleum-derived diesel fuel: application of a composition and enthalpy explicit distillation curve method. Energy Fuels 2008;22:2861–8.
[26] Smith BL, Ott LS, Bruno TJ. Composition-explicit distillation curves of diesel fuel with glycol ether and glycol ester oxygenates: fuel analysis metrology to enable decreased particulate emissions. Environ Sci Technol 2008;42:7682–9.
[27] Smith BL, Ott LS, Bruno TJ. Composition-explicit distillation curves of commercial biodiesel fuels: comparison of petroleum-derived fuel with B20 and B100. Ind Eng Chem Res 2008;47:5832–40.
[28] Bruno TJ, Wolk A, Naydich A, Huber ML. Composition-explicit distillation curves for mixtures of diesel fuel with dimethyl carbonate and diethyl carbonate. Energy Fuels 2009;23:3989–97.
[29] Windom BC, Lovestead TM, Mascal M, Nikitin EB, Bruno TJ. Advanced distillation curve analysis on ethyl levulinate as a diesel fuel oxygenate and a hybrid biodiesel fuel. Energy Fuels 2011;25:1878–90.
[30] Hsieh PY, Abel KR, Bruno TJ. Analysis of marine diesel fuel with the advanced distillation curve method. Energy Fuels 2013;27:804–10.
[31] Smith BL, Bruno TJ. Improvements in the measurement of distillation curves. 3. Application to gasoline and gasoline plus methanol mixtures. Ind Eng Chem Res 2007;46:297–309.
[32] Bruno TJ, Wolk A, Naydich A. Composition-explicit distillation curves for mixtures of gasoline with four-carbon alcohols [Butanols]. Energy Fuels 2009;23:2295–306.
[33] Bruno TJ, Wolk A, Naydich A. Analysis of fuel ethanol plant liquor with the composition explicit distillation curve method. Energy Fuels 2009;23:3277–84.
[34] Ott LS, Hadler AB, Bruno TJ. Variability of the rocket propellants RP-1, RP-2, and TS-5: application of a composition- and enthalpy-explicit distillation curve method. Ind Eng Chem Res 2008;47:9225–33.
[35] Lovestead TM, Bruno TJ. Comparison of the hypersonic vehicle fuel JP-7 to the rocket propellants RP-1 and RP-2 with the advanced distillation curve method. Energy Fuels 2009;23:3637–44.
[36] Lovestead TM, Windom BC, Riggs JR, Nickell C, Bruno TJ. Assessment of the compositional variability of RP-1 and RP-2 with the advanced distillation curve approach. Energy Fuels 2010;24:5611–23.
[37] Ott LS, Bruno TJ. Corrosivity of fluids as a function of the distillate cut: application of an advanced distillation curve method. Energy Fuels 2007;21:2778–84.
[38] Ott LS, Bruno TJ. Modifications to the copper strip corrosion test for the measurement of sulfur-related corrosion. J Sulfur Chem 2007;28:493–504.
[39] Ott LS, Smith BL, Bruno TJ. Advanced distillation curve measurements for corrosive fluids: application to two crude oils. Fuel 2008;87:3055–64.
[40] Ott LS, Smith BL, Bruno TJ. Advanced distillation curve measurement: application to a bio-derived crude oil prepared from swine manure. Fuel 2008;87:3379–87.
[41] Huber ML, Smith BL, Ott LS, Bruno TJ. Surrogate mixture model for the thermophysical properties of synthetic aviation fuel S-8: explicit application of the advanced distillation curve. Energy Fuels 2008;22:1104–14.
[42] Huber ML, Lemmon EW, Diky V, Smith BL, Bruno TJ. Chemically authentic surrogate mixture model for the thermophysical properties of a coal-derived liquid fuel. Energy Fuels 2008;22:3249–57.
[43] Huber AL, Lemmon EW, Ott LS, Bruno TJ. Preliminary surrogate mixture models for the thermophysical properties of rocket propellants RP-1 and RP-2. Energy Fuels 2009;23:3083–8.
[44] Bruno TJ, Huber ML. Evaluation of the physicochemical authenticity of aviation kerosene surrogate mixtures. Part 2: analysis and prediction of thermophysical properties. Energy Fuels 2010;24:4277–84.
[45] Huber ML, Lemmon EW, Bruno TJ. Surrogate mixture models for the thermophysical properties of aviation fuel Jet-A. Energy Fuels 2010;24:3565–71.
[46] Mueller CJ, Cannella WJ, Bruno TJ, Bunting B, Dettman HD, Franz JA, et al. Methodology for formulating diesel surrogate fuels with accurate compositional, ignition-quality, and volatility characteristics. Energy Fuels 2012;26:3284–303.

[47] He BJ, Zhang Y, Funk TL, Riskowski GL, Yin Y. Thermochemical conversion of swine manure: an alternative process for waste treatment and renewable energy production. T Asae 2000;43:1827–33.
[48] He BJ, Zhang Y, Yin Y, Funk TL, Riskowski GL. Preliminary characterization of raw oil products from the thermochemical conversion of swine manure. T Asae 2001;44:1865–71.
[49] Zhang Q, Chang J, Wang TJ, Xu Y. Review of biomass pyrolysis oil properties and upgrading research. Energy Convers Manage 2007;48:87–92.
[50] He BJ, Zhang Y, Yin Y, Funk TL, Riskowski GL. Operating temperature and retention time effects on the thermochemical conversion process of swine manure. T Asae 2000;43:1821–5.
[51] Windom BC, Bruno TJ. Improvements in the measurement of distillation curves. 5. Reduced pressure advanced distillation curve method. Ind Eng Chem Res 2011;50:1115–26.
[52] Bruno TJ, Svoronos PDN. Handbook of basic tables for chemical analysis. 3rd ed. Boca Raton: Taylor & Francis; 2011.
[53] Stein SE, Babushok VI, Brown RL, Linstrom PJ. Estimation of Kovats retention indices using group contributions. J Chem Inf Model 2007;47:975–80.
[54] Lemmon EW, Huber ML, McLinden MO. NIST standard reference database 23, NIST reference fluid thermodynamic and transport properties database (REFPROP): standard reference data. Gaithersburg, MD: National Institute of Standards and Technology; 2007.
[55] Wagner W, Pruss A. The IAPWS formulation for the thermodynamic properties of ordinary water substance for general and scientific use. J Phys Chem Ref Data 1995;31(2002):387–535.
[56] Riazi MR. Characterization and properties of petroleum fractions. West Conshohocken, PA: ASTM International; 2005.
[57] Nolte MW, Liberatore MW. Viscosity of biomass pyrolysis oils from various feedstocks. Energy Fuels 2010;24:6601–8.

Please cite this article in press as: Hsieh PY, Bruno TJ. Pressure-controlled advanced distillation curve analysis and rotational viscometry of swine manure pyrolysis oil. Fuel (2014), http://dx.doi.org/10.1016/j.fuel.2014.04.039